

Article

Generalized Logotropic Models and Their Cosmological Constraints

Hachemi Benaoum ¹ , Pierre-Henri Chavanis ^{2,*} and Hernando Quevedo ^{3,4}

¹ Department of Applied Physics and Astronomy, University of Sharjah, Sharjah P.O. Box 27272, United Arab Emirates

² Laboratoire de Physique Théorique, Université de Toulouse, CNRS, UPS, 31062 Toulouse, France

³ Instituto de Ciencias Nucleares, Universidad Nacional Autónoma de México, AP 70543, Ciudad de México 04510, Mexico

⁴ Dipartimento di Fisica and ICRA Net, Università di Roma “La Sapienza”, I-00185 Roma, Italy

* Correspondence: chavanis@irsamc.ups-tlse.fr

Abstract: We propose a new class of cosmological unified dark sector models called “Generalized Logotropic Models”. They depend on a free parameter n . The original logotropic model is a special case of our generalized model corresponding to $n = 1$. The Λ CDM model is recovered for $n = 0$. In our scenario, the Universe is filled with a single fluid, a generalized logotropic dark fluid (GLDF), whose pressure P includes higher order logarithmic terms of the rest-mass density ρ_m . The total energy density ϵ is the sum of the rest-mass energy density $\rho_m c^2$ and the internal energy density u which play the roles of dark matter energy density ϵ_m and dark energy density ϵ_{de} , respectively. We investigate the cosmological behavior of the generalized logotropic models by focusing on the evolution of the energy density, scale factor, equation of state parameter, deceleration parameter and squared speed of sound. Low values of $n \leq 3$ are favored. We also study the asymptotic behavior of the generalized logotropic models. In particular, we show that the model presents a phantom behavior and has three distinct ways of evolution depending on the value of n . For $0 < n \leq 2$, it leads to a little rip and for $n > 2$ to a big rip. We predict the value of the big rip time as a function of n without any free (undetermined) parameter.

Keywords: dark energy theory; dark matter theory; cosmology; unified dark sector; logotropic model



Citation: Benaoum, H.; Chavanis, P.-H.; Quevedo, H. Generalized Logotropic Models and Their Cosmological Constraints. *Universe* **2022**, *8*, 468. <https://doi.org/10.3390/universe8090468>

Academic Editor: Antonino Del Popolo

Received: 30 July 2022

Accepted: 31 August 2022

Published: 8 September 2022

Publisher’s Note: MDPI stays neutral with regard to jurisdictional claims in published maps and institutional affiliations.



Copyright: © 2022 by the authors. Licensee MDPI, Basel, Switzerland. This article is an open access article distributed under the terms and conditions of the Creative Commons Attribution (CC BY) license (<https://creativecommons.org/licenses/by/4.0/>).

1. Introduction

Cosmological observations from various independent research teams show that the current Universe is accelerating [1–5]. This accelerating expansion is due to an unknown component called “dark energy” which works against gravity. The nature of the dark sector is still unknown and several alternative models of dark matter (DM) and dark energy (DE) have been proposed to account for the observation of the present cosmic acceleration. The standard cold dark matter (Λ CDM) model is the simplest DE model and relies on a cosmological constant to drive the current acceleration of the Universe and on the existence of a pressureless DM to explain the observed properties of the large-scale structures of the Universe [6,7]. However, the Λ CDM model suffers from the cosmological constant problem [8,9], namely why the value of the cosmological constant is so tiny, and the cosmic coincidence problem [10,11], namely why DM and DE are of similar magnitudes today although they scale differently with the Universe’s expansion. The CDM model also faces important problems at the scale of DM halos such as the core-cusp problem [12], the missing satellite problem [13–15], and the “too big to fail” problem [16]. This leads to the so-called small-scale crisis of CDM [17]. Among the wide range of alternative DE models that have been proposed in the literature (quintessence, k-essence, Chaplygin gas, tachyons, phantom fields, holography...), an interesting class of dynamical DE models considers DM and DE as different manifestations of a single-component underlying fluid, often assumed to be a

perfect fluid. The unified dark matter and dark energy (UDM) models have the remarkable feature of describing the dark sector of the Universe as a single component that behaves as DM at early times and as DE at late times [18–38]. The cosmological aspects of these UDM models have been studied recently in refs. [34,37–42]. In particular, the logotropic model is a candidate for unifying DE and DM [30]. The logotropic model is able to account for the transition between a DM era and a DE era and is indistinguishable from the Λ CDM model, for what concerns the evolution of the cosmological background, up to 25 billion years in the future when it becomes phantom [30,31,35,40]. Remarkably, the logotropic model implies that DM halos should have a constant surface density and it predicts its universal value $\Sigma_0^{\text{th}} = 0.01955c\sqrt{\Lambda}/G = 133 M_\odot/\text{pc}^2$ [30,31,35,40] without adjustable parameter. This theoretical value is in good agreement with the value $\Sigma_0^{\text{obs}} = 141_{-52}^{+83} M_\odot/\text{pc}^2$ obtained from the observations [43]. The logotropic model also predicts the values of the present proportions of DM and DE $\Omega_{dm,0} = \frac{1}{1+e}(1 - \Omega_{b,0}) = 0.256$ and $\Omega_{de,0} = \frac{e}{1+e}(1 - \Omega_{b,0}) = 0.695$ [35,44], in good agreement with the observed values $\Omega_{dm,0} = 0.259$, $\Omega_{de,0} = 0.691$ and $\Omega_{b,0} = 0.0486$.

In this work, we introduce a new class of UDM models called “Generalized Logotropic Models” characterized by a single fluid equation of state (EoS) of the form

$$P = \sum_{i=0}^N A_i \ln^i \left(\frac{\rho_m}{\rho_P} \right), \tag{1}$$

where P is the pressure, ρ_m is the rest-mass density, A_i are constants with the dimension of an energy density and ρ_P is a constant with the dimension of a mass density. The above EoS returns the standard Λ CDM model for $N = 0$ and the original logotropic model [30] for $N = 1$. Following [30], we shall identify ρ_P with the Planck density $\rho_P = c^5/(\hbar G^2) = 5.16 \times 10^{99} \text{ g m}^{-3}$. The single fluid which obeys Equation (1) will be called the generalized logotropic dark fluid (GLDF).

In this paper, we are interested in studying the dynamical evolution of various generalized logotropic models. In particular, we examine in detail various forms of generalized logotropic EoS and investigate how the Universe’s evolution is affected by the corresponding EoS. In Section 2, we provide an approach to motivate the logotropic model. In Section 3, we consider an isotropic, homogeneous and spatially flat Universe and introduce the main equations characterizing generalized logotropic models. In Section 4, we consider a subclass of models with $A_i = A_n \delta_{i,n}$ that are more easily tractable. In Section 5, we investigate the cosmological behavior of the generalized logotropic models and focus on the evolution of the energy density, scale factor, EoS parameter, deceleration parameter and squared speed of sound. We also derive analytically the asymptotic behavior of the generalized logotropic models and distinguish three types of evolution depending on the value of n . Finally, Section 6 is devoted to remarks and conclusions. In Appendix A, we show that the GLDF is asymptotically equivalent to a form of Modified Chaplygin Gas (MCG). In Appendix B, we consider the two-fluid model associated with the GLDF and determine the EoS of DE. In Appendix C, we derive the present proportions of DM and DE by taking into account the presence of baryons.

2. Generalized Logotropic Equation of State

We consider the scenario where both DM and DE originate from a single dark fluid. We first recall the justification of the standard logotropic equation of state given in [30]. In the Newtonian regime, the condition of hydrostatic equilibrium, which describes the balance between the gravitational force and the pressure gradient, is given by

$$\nabla P + \rho \nabla \Phi = \mathbf{0}. \tag{2}$$

Here, P and ρ denote the pressure and mass density of the fluid, respectively. Moreover, Φ is the gravitational potential. We assume one of the simplest direct relations between the mass density ρ and the pressure P of the fluid given by the polytropic EoS

$$P = K\rho^\gamma, \tag{3}$$

where γ is the polytropic index and K is a constant. Using the above equation, the condition of hydrostatic equilibrium becomes

$$K\gamma\rho^{\gamma-1}\nabla\rho + \rho\nabla\Phi = \mathbf{0}. \tag{4}$$

Considering the limit $\gamma \rightarrow 0, K \rightarrow +\infty$ with $A = K\gamma$ fixed [30], we obtain

$$A\frac{\nabla\rho}{\rho} + \rho\nabla\Phi = \mathbf{0}. \tag{5}$$

By comparing Equations (5) and (2), we find that the EoS of the logotropic gas reads [30]

$$P = A \ln\left(\frac{\rho}{\rho_*}\right), \tag{6}$$

where ρ_* is an integration constant. In this paper, we consider a generalization of this EoS of the form

$$P = \sum_{i=0}^N A_i \ln^i\left(\frac{\rho}{\rho_*}\right), \tag{7}$$

where A_i are arbitrary constants. This generalized logotropic EoS is interesting in its own right and, as we shall see, it possesses interesting properties. However, the above derivation suggests that the standard logotropic EoS (6) plays a special role in the problem.

Remark 1. *The logotropic model was originally introduced with the following motivation [30]. The Λ CDM model can be viewed as a UDM model with a constant pressure $P = -\rho_\Lambda c^2$, where $\rho_\Lambda = \Lambda/(8\pi G) = 5.96 \times 10^{-24} \text{ g m}^{-3}$ is the cosmological density. This corresponds to the equation of state (3) with $\gamma = 0$ and $K = -\rho_\Lambda c^2 < 0$. The Λ CDM model works well at large (cosmological) scales but experiences some problems at small (galactic) scales such as the core-cusp problem and the missing satellite problem. The small-scale crisis of the Λ CDM model is related to the fact that there is no pressure force ($\nabla P = \mathbf{0}$) to balance the gravitational attraction. The idea is therefore to introduce a model that is as close as possible to the Λ CDM model but that has $\nabla P \neq \mathbf{0}$. Such a model should have $\gamma \simeq 0$. An idea would be to take $\gamma = \eta > 0$ (with $\eta \ll 1$) and a given value of K but we recover the drawbacks of the Λ CDM when η is sufficiently small. Another possibility is to take $\gamma \rightarrow 0$ and $K \rightarrow \infty$ in such a way that $A = K\gamma$ is fixed. This leads to the logotropic equation of state (6) which has $\nabla P \neq \mathbf{0}$. A logarithm is the closest function to a constant that has a gradient. Interestingly, the logotropic equation of state gives a mathematical meaning to the self-gravitating polytrope of index $n = -1$ which is otherwise ill-defined [45]. Therefore, the logotropic equation of state nicely completes the family of polytropic equations of state by filling the gap at $n = -1$ [46]. Furthermore, it is the only equation of state that leads to DM halos with a universal surface density, in agreement with the observations [30].*

3. Generalized Logotropic Cosmology

In this section, we consider a flat homogeneous and isotropic Friedmann–Lemaître–Robertson–Walker (FLRW) universe filled with a perfect single fluid, having an energy density ϵ , rest-mass density ρ_m , and pressure P . The expansion dynamics are governed by the Friedmann equations [47]

$$H^2 = \left(\frac{\dot{a}}{a}\right)^2 = \frac{8\pi G}{3c^2}\epsilon, \tag{8}$$

$$\dot{H} + H^2 = \frac{\ddot{a}}{a} = -\frac{4\pi G}{3c^2}(\epsilon + 3P), \tag{9}$$

where $a(t)$ is the scale factor and $H = \dot{a}/a$ is the Hubble parameter. Combining Equations (8) and (9), we obtain the energy conservation equation

$$\frac{d\epsilon}{dt} + 3H(\epsilon + P) = 0. \tag{10}$$

For a relativistic fluid with an adiabatic evolution (or at $T = 0$), the first law of thermodynamics reduces to

$$d\epsilon = \frac{P + \epsilon}{\rho_m} d\rho_m. \tag{11}$$

By integrating this equation for a given EoS, $P = P(\rho_m)$, a relation between the energy density and the rest-mass density can be obtained as [30]

$$\epsilon = \rho_m c^2 + \rho_m \int^{\rho_m} \frac{P(\rho')}{\rho'^2} d\rho' = \rho_m c^2 + u(\rho_m), \tag{12}$$

where $\rho_m c^2$ is the rest-mass energy density and u is the internal energy density. For our generalized logotropic model with an EoS given by Equation (1), we obtain

$$\epsilon = \rho_m c^2 - \sum_{i=0}^N A_i I_i(\rho_m) \tag{13}$$

with the integral $I_i(\rho_m)$ given by

$$I_i(\rho_m) = \rho_m \int_{\rho_m}^{+\infty} \ln^i\left(\frac{\rho'_m}{\rho_P}\right) \frac{d\rho'_m}{\rho_m'^2}. \tag{14}$$

With the change of variables $y = \ln(\rho'_m/\rho_P)$, we obtain

$$I_i(\rho_m) = \frac{\rho_m}{\rho_P} \int_{\ln(\rho_m/\rho_P)}^{+\infty} y^i e^{-y} dy. \tag{15}$$

In terms of the incomplete gamma function

$$\Gamma(\alpha + 1, x) = \int_x^{+\infty} y^\alpha e^{-y} dy \tag{16}$$

the integral $I_i(\rho_m)$ can be rewritten as

$$I_i(\rho_m) = \frac{\rho_m}{\rho_P} \Gamma\left[i + 1, \ln\left(\frac{\rho_m}{\rho_P}\right)\right] = i! \sum_{k=0}^i \frac{1}{k!} \ln^k\left(\frac{\rho_m}{\rho_P}\right). \tag{17}$$

To obtain the second equality, we have used the relation

$$\Gamma(n + 1, x) = n! e^{-x} \sum_{k=0}^n \frac{1}{k!} x^k, \tag{18}$$

which can be obtained by computing $\partial\Gamma(n + 1, x)/\partial x$ from Equations (16) and (18). For future purposes, we note the asymptotic behavior ¹

$$\Gamma(n + 1, x) \sim x^n e^{-x} \quad (x \rightarrow \infty). \tag{19}$$

The energy density can then be written as

$$\epsilon = \rho_m c^2 - \sum_{i=0}^N A_i \frac{\rho_m}{\rho_P} \Gamma \left[i + 1, \ln \left(\frac{\rho_m}{\rho_P} \right) \right]. \tag{20}$$

Equations (1) and (20) determine the EoS $P(\epsilon)$ in parametric form. By combining the energy conservation Equation (10) with the first law of thermodynamics (11) one finds that the rest-mass density evolves as [30]

$$\frac{d\rho_m}{dt} + 3H\rho_m = 0 \quad \Rightarrow \quad \rho_m = \frac{\rho_{m,0}}{a^3}, \tag{21}$$

where $\rho_{m,0} = \rho_m(a_0 = 1)$ is the present value of the rest-mass density and $a_0 = 1$ is the present value of the scale factor. Equation (21) expresses the conservation of the rest-mass. On the other hand, the internal energy is given by

$$u = - \sum_{i=0}^N A_i I_i(\rho_m) = - \sum_{i=0}^N A_i I_i \left(\frac{\rho_{m,0}}{a^3} \right). \tag{22}$$

As argued in [30], the rest-mass energy density $\rho_m c^2$ plays the role of pressureless DM ($\epsilon_m = \rho_m c^2$) and the internal energy u plays the role of DE ($\epsilon_{de} = u$)². The energy density $\epsilon = \epsilon_m + \epsilon_{de}$ of the generalized logotropic model is therefore the sum of two terms where the first term ϵ_m can be interpreted as the DM energy density given by

$$\epsilon_m = \frac{\epsilon_{m,0}}{a^3} \tag{23}$$

and the second term ϵ_{de} can be interpreted as the DE energy density given by

$$\epsilon_{de} = - \frac{e^{-1-1/B}}{a^3} \sum_{i=0}^N A_i \Gamma \left(i + 1, -1 - \frac{1}{B} - 3 \ln a \right), \tag{24}$$

where, following [30], we have defined the dimensionless parameter B through the relation

$$\frac{\rho_P}{\rho_{m,0}} = e^{1+1/B}. \tag{25}$$

The Friedmann Equation (8) can be written as

$$H^2 = H_0^2 \left(\frac{\epsilon_m}{\epsilon_0} + \frac{\epsilon_{de}}{\epsilon_0} \right), \tag{26}$$

where $\epsilon_0 = 3H_0^2 c^2 / 8\pi G$ is the critical energy density and H_0 is the value of the Hubble parameter at the present time.

The pressure and the energy density of the generalized logotropic model can be expressed in terms of the scale factor as

$$P = \sum_{i=0}^N A_i \left(-1 - \frac{1}{B} - 3 \ln a \right)^i, \tag{27}$$

$$\epsilon = \frac{\Omega_{m,0} \epsilon_0}{a^3} - \frac{e^{-1-1/B}}{a^3} \sum_{i=0}^N A_i \Gamma \left(i + 1, -1 - \frac{1}{B} - 3 \ln a \right). \tag{28}$$

The present proportions of DM and DE, denoted $\Omega_{m,0}$ and $\Omega_{de,0}$, are given by

$$\Omega_{m,0} = \frac{\epsilon_{m,0}}{\epsilon_0}, \tag{29}$$

$$\Omega_{de,0} = \frac{\epsilon_{de,0}}{\epsilon_0} = -\frac{e^{-1-1/B}}{\epsilon_0} \sum_{i=0}^N A_i \Gamma\left(i + 1, -1 - \frac{1}{B}\right) = 1 - \Omega_{m,0}. \tag{30}$$

For given values of $\Omega_{m,0}$ and ϵ_0 (through H_0), which can be obtained from the observations, Equation (25) determines B and Equation (30) provides a constraint on the coefficients A_i . Using $\rho_P = c^5/(\hbar G^2) = 5.16 \times 10^{99} \text{ g m}^{-3}$ and $\rho_{m,0} = \Omega_{m,0}\epsilon_0/c^2$ with $\Omega_{m,0} = 0.309$ and $\epsilon_0/c^2 = 8.62 \times 10^{-24} \text{ g m}^{-3}$, we obtain $B = 3.53 \times 10^{-3}$. We have taken the values of $\Omega_{m,0}$ and ϵ_0 from the Λ CDM model but since B is defined by a logarithm, its value is very insensitive to the precise values of $\Omega_{m,0}$ and ϵ_0 . Therefore, the value $B = 3.53 \times 10^{-3}$ is very robust [31].

In the late Universe ($a \rightarrow \infty$ and $\rho_m \rightarrow 0$), the DE dominates and, using Equation (19), we obtain $\epsilon \sim -A_N(-3 \ln a)^N$ and $P \sim A_N(-3 \ln a)^N$, which implies that the EoS $P(\epsilon)$ behaves asymptotically as $P/\epsilon \rightarrow -1$. We note that in order to have $\epsilon > 0$ when $a \rightarrow +\infty$, the parameter A_N must be negative if N is even and positive if N is odd. Below we present some interesting UDM models derived from the generalized logotropic model, focusing on the EoS $P(\epsilon)$, the energy density ϵ and the cosmological implications of these models. We also investigate the era of DE dominance that drives the accelerated expansion of the Universe.

4. Particular Models

4.1. The Case $A_i = A_n \delta_{i,n}$

This case focuses on just the n -th order term of the finite series leading to the EoS

$$P = A_n \ln^n \left(\frac{\rho_m}{\rho_P} \right). \tag{31}$$

The energy density is given by

$$\epsilon = \rho_m c^2 - A_n \frac{\rho_m}{\rho_P} \Gamma \left[n + 1, \ln \left(\frac{\rho_m}{\rho_P} \right) \right] = \rho_m c^2 + u = \epsilon_m + \epsilon_{de}, \tag{32}$$

where the first term is the rest-mass energy density (DM) and the second term is the internal energy density (DE). The pressure and total energy density as a function of the scale factor reduces to

$$P = A_n \left(-1 - \frac{1}{B} - 3 \ln a \right)^n, \tag{33}$$

$$\epsilon = \frac{\Omega_{m,0}\epsilon_0}{a^3} - A_n \frac{e^{-1-1/B}}{a^3} \Gamma \left(n + 1, -1 - \frac{1}{B} - 3 \ln a \right). \tag{34}$$

At the present time (i.e., $a = 1$), the above equation leads to

$$A_n = -\frac{(1 - \Omega_{m,0})\epsilon_0 e^{1+1/B}}{\Gamma \left(n + 1, -1 - \frac{1}{B} \right)}, \tag{35}$$

which determines A_n as a function of the measured values of $\Omega_{m,0}$ and ϵ_0 . The dimensionless constant B is also determined by the measured values of $\Omega_{m,0}$ and ϵ_0 (see above). As a result, there is no free parameter in this model³. Note that

$$\frac{A_n}{(1 - \Omega_{m,0})\epsilon_0} = -\frac{e^{1+1/B}}{\Gamma \left(n + 1, -1 - \frac{1}{B} \right)} \tag{36}$$

is a dimensionless constant depending only on n and B . Furthermore, $\rho_\Lambda \equiv (1 - \Omega_{m,0})\epsilon_0/c^2 = 5.96 \times 10^{-24} \text{ g m}^{-3}$ is the present value of the DE density (it is equal to the cosmological

density $\rho_\Lambda = \Lambda / (8\pi G)$ in the Λ CDM model). From Equation (36), we find that $A_n < 0$ for n even and $A_n > 0$ for n odd.

On the other hand, from Equation (31), the pressure P vanishes when $\rho_m = \rho_P$. If n is even, the pressure P is always negative. If n is odd, the pressure P is positive for $\rho_m > \rho_P$ and negative for $\rho_m < \rho_P$. In practice, we consider a regime where $\rho_m \ll \rho_P$ because the logotropic model does not describe the early inflation. In that case, the pressure is always negative. The EoS $P(\epsilon)$ is given in the reversed form $\epsilon(P)$ by

$$\epsilon = e^{\mp \left| \frac{P}{A_n} \right|^{1/n}} \rho_P c^2 - A_n e^{\mp \left| \frac{P}{A_n} \right|^{1/n}} \Gamma \left(n + 1, \mp \left| \frac{P}{A_n} \right|^{1/n} \right), \tag{37}$$

where the upper sign corresponds to the most relevant case $\rho_m < \rho_P$ and the lower sign corresponds to $\rho_m > \rho_P$. Substituting Equation (35) into Equations (33) and (34), we obtain after simple manipulations

$$P = - \frac{(1 - \Omega_{m,0})\epsilon_0}{\Gamma \left(n + 1, -1 - \frac{1}{B} \right)} e^{1+1/B} \left(-1 - \frac{1}{B} - 3 \ln a \right)^n, \tag{38}$$

$$\epsilon = \frac{\Omega_{m,0}\epsilon_0}{a^3} + \frac{(1 - \Omega_{m,0})\epsilon_0}{a^3} \frac{\Gamma \left(n + 1, -1 - \frac{1}{B} - 3 \ln a \right)}{\Gamma \left(n + 1, -1 - \frac{1}{B} \right)}. \tag{39}$$

In the early Universe ($a \rightarrow 0, \rho_m \rightarrow +\infty$) the DM ϵ_m dominates and we have $\epsilon \sim \Omega_{m,0}\epsilon_0/a^3$, $P \sim A_n(-3 \ln a)^n$ such that $P/\epsilon \rightarrow 0$ whereas, in the late Universe ($a \rightarrow \infty, \rho_m \rightarrow 0$), the DE ϵ_{de} dominates and we have $\epsilon \sim -A_n(-3 \ln a)^n$, $P \sim A_n(-3 \ln a)^n$ such that $P/\epsilon \rightarrow -1$. Furthermore, in order to have $\epsilon > 0$ for $a \rightarrow +\infty$, the parameter A_n must be negative if n is even and positive if n is odd. As we have seen, this is guaranteed by Equation (35). Finally, it is worth mentioning that for $B \rightarrow 0$ (corresponding to a form of semiclassical limit $\rho_P \rightarrow +\infty$ or $\hbar \rightarrow 0$), the Λ CDM model is recovered [31]. Indeed, using Equation (19), we find that Equations (38) and (39) reduce to

$$P = -(1 - \Omega_{m,0})\epsilon_0, \tag{40}$$

$$\epsilon = \frac{\Omega_{m,0}\epsilon_0}{a^3} + (1 - \Omega_{m,0})\epsilon_0. \tag{41}$$

4.2. The Case $A_i = A_0 \delta_{i,0}$

For $n = 0$, we recover the Λ CDM model (interpreted as a UDM model) corresponding to the EoS

$$P = A_0. \tag{42}$$

The energy density is given by

$$\epsilon = \rho_m c^2 - A_0, \tag{43}$$

where the first term is DM and the second term is DE. The total energy density as a function of the scale factor reads

$$\epsilon = \frac{\Omega_{m,0}\epsilon_0}{a^3} - A_0. \tag{44}$$

At the present time (i.e., $a = 1$), Equation (44) leads to

$$A_0 = -(1 - \Omega_{m,0})\epsilon_0. \tag{45}$$

We note that $A_0 < 0$. Numerically, $A_0/c^2 = -\rho_\Lambda = -5.96 \times 10^{-24} \text{ g m}^{-3}$, where ρ_Λ is the cosmological density. The pressure P and the energy density ϵ are then given by Equations (40) and (41). The pressure $P = -\rho_\Lambda c^2$ is constant and negative. As the universe

expands, starting from $+\infty$, the energy density ϵ decreases and tends to a constant value $\rho_\Lambda c^2$. The DE density $\epsilon_{de} = \rho_\Lambda c^2$ is constant.

4.3. The Case $A_i = A_1 \delta_{i,1}$

For $n = 1$, we recover the original logotropic model [30] corresponding to the EoS

$$P = A \ln\left(\frac{\rho_m}{\rho_P}\right), \tag{46}$$

where we have denoted $A_1 = A$. The energy density is given by

$$\epsilon = \rho_m c^2 - A \left[1 + \ln\left(\frac{\rho_m}{\rho_P}\right) \right], \tag{47}$$

where the first term is DM and the second term is DE. The EoS $P(\epsilon)$ is given in the reversed form $\epsilon(P)$ by

$$\epsilon = e^{P/A} \rho_P c^2 - A - P. \tag{48}$$

The pressure and total energy density as a function of the scale factor read

$$P = -A \left(1 + \frac{1}{B} + 3 \ln a \right), \tag{49}$$

$$\epsilon = \frac{\Omega_{m,0} \epsilon_0}{a^3} + A \left(\frac{1}{B} + 3 \ln a \right). \tag{50}$$

At the present time (i.e., $a = 1$), Equation (50) leads to

$$A = B(1 - \Omega_{m,0})\epsilon_0. \tag{51}$$

We note that $A > 0$. Numerically, $A/c^2 = B\rho_\Lambda = 3.53 \times 10^{-3} \rho_\Lambda = 2.10 \times 10^{-26} \text{ g m}^{-3}$. The pressure P and the energy density ϵ become

$$P = -(1 - \Omega_{m,0})\epsilon_0(B + 1 + 3B \ln a), \tag{52}$$

$$\epsilon = \frac{\Omega_{m,0} \epsilon_0}{a^3} + (1 - \Omega_{m,0})\epsilon_0(1 + 3B \ln a). \tag{53}$$

The pressure P is positive when $\rho_m > \rho_P$ and negative when $\rho_m < \rho_P$. It vanishes at $\rho_m = \rho_P$. As the universe expands, the pressure decreases from $+\infty$ to $-\infty$. Starting from $+\infty$, the energy density ϵ first decreases, reaches a minimum $\epsilon_{\min} = A \ln(\rho_P c^2 / A) > 0$ at $\rho_m = A/c^2$, then increases to $+\infty$. The DE density ϵ_{de} increases from $-\infty$ to $+\infty$. The DE is negative when $\rho_m > \rho_P/e$ and positive when $\rho_m < \rho_P/e$ (its value at $\rho_m = \rho_P$ is $\epsilon_{de} = -A < 0$). In the logotropic model, since the DE density corresponds to the internal energy density u of the LDF, it can very well be negative as long as the total energy density ϵ is positive. Note, however, that in the regime of interest $\rho_m \ll \rho_P$, the DE density ϵ_{de} is positive.

4.4. The Case $A_i = A_2 \delta_{i,2}$

For $n = 2$, we obtain the EoS

$$P = A_2 \ln^2\left(\frac{\rho_m}{\rho_P}\right). \tag{54}$$

The energy density is given by

$$\epsilon = \rho_m c^2 - 2A_2 \left[1 + \ln\left(\frac{\rho_m}{\rho_P}\right) + \frac{1}{2} \ln^2\left(\frac{\rho_m}{\rho_P}\right) \right], \tag{55}$$

where the first term is DM and the second term is DE. The EoS $P(\epsilon)$ is given in the reversed form $\epsilon(P)$ by

$$\epsilon = e^{\mp \sqrt{\frac{P}{A_2}}} \rho_P c^2 - 2A_2 \left(1 \mp \sqrt{\frac{P}{A_2} + \frac{1}{2} \frac{P}{A_2}} \right), \tag{56}$$

where the upper sign corresponds to the most relevant case $\rho_m < \rho_P$ and the lower sign corresponds to $\rho_m > \rho_P$. The pressure and total energy density as a function of the scale factor read

$$P = A_2 \left(1 + \frac{1}{B} + 3 \ln a \right)^2, \tag{57}$$

$$\epsilon = \frac{\Omega_{m,0} \epsilon_0}{a^3} - 2A_2 \left[-\frac{1}{B} - 3 \ln a + \frac{1}{2} \left(1 + \frac{1}{B} + 3 \ln a \right)^2 \right]. \tag{58}$$

At the present time (i.e., $a = 1$), Equation (58) leads to

$$A_2 = -\frac{1 - \Omega_{m,0}}{1 + \frac{1}{B^2}} \epsilon_0. \tag{59}$$

We note that $A_2 < 0$. Numerically, $A_2/c^2 = -B^2/(1 + B^2)\rho_\Lambda = -1.25 \times 10^{-5}\rho_\Lambda = 7.43 \times 10^{-29} \text{ g m}^{-3}$. The pressure P and the energy density ϵ become

$$P = -\frac{(1 - \Omega_{m,0})\epsilon_0}{1 + B^2} (1 + B + 3B \ln a)^2, \tag{60}$$

$$\epsilon = \frac{\Omega_{m,0}\epsilon_0}{a^3} + (1 - \Omega_{m,0})\epsilon_0 \frac{1 + B^2 + 6B \ln a + 9B^2 \ln^2 a}{1 + B^2}. \tag{61}$$

The pressure P is always negative and vanishes at $\rho_m = \rho_P$. As the universe expands, starting from $-\infty$, the pressure first increases, vanishes at $\rho = \rho_m$, then decreases to $-\infty$. Starting from $+\infty$, the energy density ϵ first decreases, reaches a minimum $\epsilon_{\min} = -A_2(\rho_m c^2/2A_2 - 1)^2 > 0$ at ρ_m solution of $\rho_m c^2 = 2A_2[1 + \ln(\rho_m/\rho_P)]$, then increases to $+\infty$. Starting from $+\infty$, the DE density ϵ_{de} first decreases, reaches a minimum $\epsilon_{de}^{\min} = -A_2 > 0$ at $\rho_m = \rho_P/e$, then increases to $+\infty$ (its value at $\rho_m = \rho_P$ is $\epsilon_{de} = -2A_2 > 0$).

Cases with $n = 1, 2$ are the simplest logotropic models. Since n is a free parameter, cases with $n > 2$ lead to a collection of generalized logotropic models.

4.5. The Case $N = 2$

This generalized logotropic model is obtained by considering the first three terms A_0 , A_1 and A_2 . This leads to the EoS

$$P = A_0 + A_1 \ln\left(\frac{\rho_m}{\rho_P}\right) + A_2 \ln^2\left(\frac{\rho_m}{\rho_P}\right). \tag{62}$$

The energy density is given by

$$\epsilon = \rho_m c^2 - A_0 - A_1 \left[1 + \ln\left(\frac{\rho_m}{\rho_P}\right) \right] - 2A_2 \left[1 + \ln\left(\frac{\rho_m}{\rho_P}\right) + \frac{1}{2} \ln^2\left(\frac{\rho_m}{\rho_P}\right) \right], \tag{63}$$

where the first term is DM and the other terms are DE. The EoS $P(\epsilon)$ can be obtained in the reversed form $\epsilon(P)$ by eliminating ρ_m between Equations (62) and (63)⁴. The pressure and the energy density evolve with the scale factor as

$$P = A_0 + A_1 \left(-1 - \frac{1}{B} - 3 \ln a \right) + A_2 \left(-1 - \frac{1}{B} - 3 \ln a \right)^2, \tag{64}$$

$$\epsilon = \frac{\Omega_{m,0}\epsilon_0}{a^3} - A_0 + A_1 \left(\frac{1}{B} + 3 \ln a \right) - 2A_2 \left[-\frac{1}{B} - 3 \ln a + \frac{1}{2} \left(1 + \frac{1}{B} + 3 \ln a \right)^2 \right]. \tag{65}$$

At the present time (i.e., $a = 1$), the above equation gives

$$(1 - \Omega_{m,0}) \epsilon_0 = -A_0 + \frac{A_1}{B} - A_2 \left(1 + \frac{1}{B^2} \right), \tag{66}$$

which constrains one of the three free parameters. As a result, the model has only two free parameters. As expected, in the late Universe ($a \rightarrow \infty, \rho_m \rightarrow 0$), the DE density ϵ_{de} dominates and we have $P/\epsilon \rightarrow -1$. It is worth mentioning that in order to have $\epsilon > 0$, A_2 must be negative.

5. Evolution of the Generalized Logotropic Model

In the following we consider models with $A_i = A_n \delta_{i,n}$. The evolution of the energy density as a function of the scale factor [see Equation (39)] is plotted in Figure 1, where we have used the best-fit values of the parameters $\Omega_{m,0} = 0.309$ and $B = 3.53 \times 10^{-3}$ obtained from the Λ CDM model (they are consistent with the cosmological analysis of the original logotropic model [40,41]). The Universe starts at $a = 0$ with an infinite energy density⁵. The energy density ϵ first decreases with the increase in the scale factor a , reaches a minimum, then increases with the scale factor characterizing a phantom Universe [48,49].

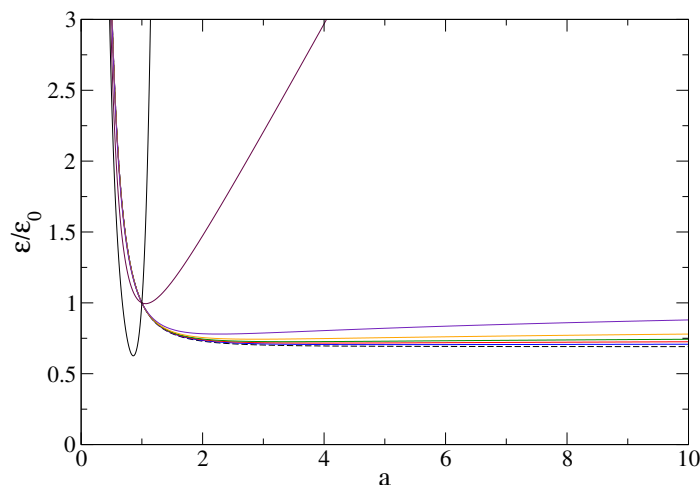


Figure 1. Normalized energy density ϵ/ϵ_0 as a function of the scale factor a for $\Omega_{m,0} = 0.309$, $B = 3.53 \times 10^{-3}$ and various values of n : $n = 0$ (dashed black, Λ CDM model), $n = 1$ (blue, original logotropic model), $n = 2$ (red), $n = 3$ (green), $n = 5$ (orange), $n = 10$ (indigo), $n = 100$ (maroon), $n = 1000$ (black).

In the generalized logotropic model, the Friedmann Equation (26) takes the form

$$H = \frac{\dot{a}}{a} = H_0 \sqrt{\frac{\Omega_{m,0}}{a^3} + \frac{1 - \Omega_{m,0}}{a^3} \frac{\Gamma\left(n + 1, -1 - \frac{1}{B} - 3 \ln a\right)}{\Gamma\left(n + 1, -1 - \frac{1}{B}\right)}}. \tag{67}$$

The evolution of the scale factor as a function of the time is given by

$$H_0 t = \int_0^a \frac{da'}{a' \sqrt{\frac{\Omega_{m,0}}{a'^3} + \frac{1-\Omega_{m,0}}{a'^3} \frac{\Gamma(n+1, -1-\frac{1}{B}-3 \ln a')}{\Gamma(n+1, -1-\frac{1}{B})}}}. \tag{68}$$

The Λ CDM model is recovered from Equation (68) for $n = 0$ or $B = 0$. In that case, Equation (68) can be integrated analytically yielding

$$a = \left(\frac{\Omega_{m,0}}{1 - \Omega_{m,0}} \right)^{1/3} \sinh^{2/3} \left(\frac{3}{2} \sqrt{1 - \Omega_{m,0}} H_0 t \right), \tag{69}$$

$$\frac{\epsilon}{\epsilon_0} = \frac{1 - \Omega_{m,0}}{\tanh^2 \left(\frac{3}{2} \sqrt{1 - \Omega_{m,0}} H_0 t \right)}, \tag{70}$$

whereas for $B \neq 0$ it can only be integrated numerically. Figure 2 shows the behavior of the scale factor a as a function of t for $n = 0, 1, 2, 3, 5, 10, 100, 1000$. The age of the universe (corresponding to $a = 1$) is given by

$$t_{\text{age}} = \frac{1}{H_0} \int_0^1 \frac{da'}{a' \sqrt{\frac{\Omega_{m,0}}{a'^3} + \frac{1-\Omega_{m,0}}{a'^3} \frac{\Gamma(n+1, -1-\frac{1}{B}-3 \ln a')}{\Gamma(n+1, -1-\frac{1}{B})}}}. \tag{71}$$

with $H_0 = 2.195 \times 10^{-18} \text{ s}^{-1}$, i.e., $H_0^{-1} = 14.4 \text{ Gyrs}$. For the Λ CDM model ($n = 0$) we recover the well-known result $t_{\text{age}} = 0.956 H_0^{-1} = 13.8 \text{ Gyrs}$. A difference larger than 0.1% (the typical error bar on the age of the universe) occurs in models with $n > 3$ so these models should be rejected⁶. For example, we obtain $t_{\text{age}} = 0.966 H_0^{-1} = 13.9 \text{ Gyrs}$ for $n = 20$, $t_{\text{age}} = 0.998 H_0^{-1} = 14.4 \text{ Gyrs}$ for $n = 100$, and $t_{\text{age}} = 1.12 H_0^{-1} = 16.1 \text{ Gyrs}$ for $n = 1000$.

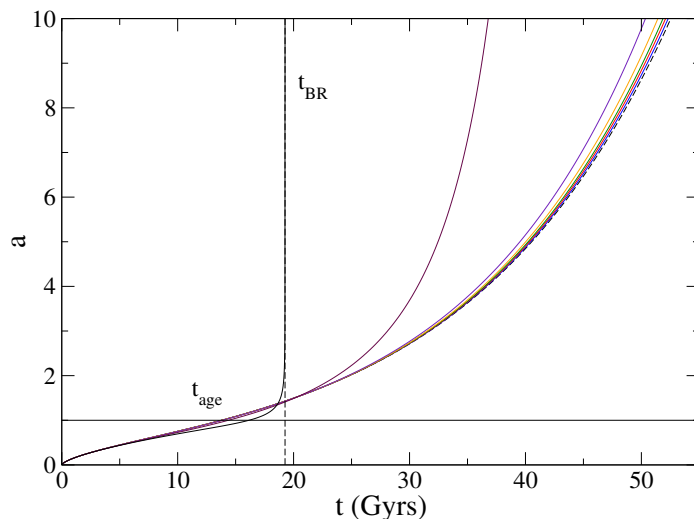


Figure 2. Scale factor a as a function of the cosmic time t for $\Omega_{m,0} = 0.309$, $B = 3.53 \times 10^{-3}$ and $n = 0, 1, 2, 3, 5, 10, 100, 1000$. This figure shows the big rip time t_{BR} (for $n = 1000 > 2$) at which the scale factor becomes infinite.

The asymptotic behavior of the generalized logotropic model can be obtained analytically. For $a \rightarrow 0$, we have a matter-dominated Universe which corresponds to Einstein-deSitter (EdS) solution given by

$$a \sim \left(\frac{3}{2}\sqrt{\Omega_{m,0}}H_0t\right)^{2/3}, \tag{72}$$

$$\frac{\epsilon}{\epsilon_0} \sim \frac{4}{9H_0^2t^2}. \tag{73}$$

For $a \rightarrow +\infty$, the energy density behaves as

$$\epsilon \sim 3^n|A_n|(\ln a)^n. \tag{74}$$

In this asymptotic regime, the Friedmann equation can be written as

$$\frac{\dot{a}}{a} = \sqrt{\frac{8\pi G}{3c^2}\epsilon} \sim K_n (\ln a)^{n/2}, \tag{75}$$

where we define the constant K_n as

$$K_n = 3^{n/2}H_0 \sqrt{\frac{(1 - \Omega_{m,0})e^{1+1/B}}{\Gamma\left(n + 1, -1 - \frac{1}{B}\right)}}. \tag{76}$$

The above equation can be integrated into

$$K_n t \sim \int^a \frac{da'}{a'(\ln a')^{n/2}} \sim \int^{\ln a} \frac{ds}{s^{n/2}}, \tag{77}$$

where we have made the change of variables $s = \ln a'$ to obtain the second equality. It is interesting to note that the asymptotic evolution of the scale factor as a function of time depends mainly on the value of the parameter n . We can distinguish three relevant types of evolution which correspond to $n < 2$, $n = 2$ and $n > 2$.

(i) For $n < 2$: this solution, which includes the original logotropic model [30,31,40], describes a super de Sitter evolution of the form

$$a \propto \exp\left\{\left[\frac{1}{2}(2 - n) K_n t\right]^{\frac{2}{2-n}}\right\}, \quad \epsilon \propto t^{\frac{2n}{2-n}}, \tag{78}$$

where the scale factor grows super exponentially rapidly with cosmic time causing an algebraic divergence of the energy density. For $n = 1$ we recover the original logotropic model where $a \sim e^{t^2}$ and $\epsilon \sim t^2$ [30,31,40]. Since the scale factor and the energy density increase indefinitely with time, this is called Little Rip [50]. For $n = 0$ we recover the Λ CDM model presenting an exponential (de Sitter) expansion $a \sim e^t$ and a constant energy density $\epsilon \sim 1$.

(ii) For $n = 2$: we obtain a double exponential evolution of the form

$$a \propto \exp[\exp(K_2 t)], \quad \epsilon \propto \exp(2K_2 t), \tag{79}$$

where the scale factor grows hyper exponentially rapidly with cosmic time causing an exponential divergence of the energy density (Little Rip).

(iii) For $n > 2$: this case represents a situation in which the Universe ends up with a finite-time future singularity. One finds

$$a \propto \exp \left\{ \left[\frac{1}{2} (n - 2) K_n (t_s - t) \right]^{-\frac{2}{n-2}} \right\}, \quad \epsilon \propto \left[\frac{1}{2} (n - 2) K_n (t_s - t) \right]^{-\frac{2n}{n-2}}. \quad (80)$$

The singularity at $t = t_s$ corresponds to a Big Rip [49] characterized by the divergence of the scale factor and energy density in finite time. The big rip time (corresponding to $a \rightarrow +\infty$) is given by

$$t_{BR} = \frac{1}{H_0} \int_0^{+\infty} \frac{da'}{a' \sqrt{\frac{\Omega_{m,0}}{a'^3} + \frac{1 - \Omega_{m,0}}{a'^3} \frac{\Gamma(n+1, -1 - \frac{1}{B} - 3 \ln a')}{\Gamma(n+1, -1 - \frac{1}{B})}}}. \quad (81)$$

For measured values of $\Omega_{m,0}$ and ϵ_0 (hence H_0), this is just a function of n . There is no other free (undetermined) parameter in our model. We obtain $t_{BR} = 3240$ Gyrs for $n = 3$, $t_{BR} = 1650$ Gyrs for $n = 4$, $t_{BR} = 422$ Gyrs for $n = 10$, $t_{BR} = 47.1$ Gyrs for $n = 100$, and $t_{BR} = 19.2$ Gyrs for $n = 1000$. However, we recall that the models with $n > 3$ are excluded from the observations.

We note that the expansion of the Universe at late times is faster for higher n . In particular, the big rip time (when $n > 2$) decreases with n . Still the age of the Universe (calculated at $a = 1$) slightly increases with n . Therefore, for higher n , the Universe is older than for the Λ CDM model, and not younger. This counterintuitive behavior is illustrated in Figure 2. There is no paradox since it is only *asymptotically* (for $a \rightarrow +\infty$) that the expansion of the Universe is faster for higher n . For intermediate times (around $a \sim 1$), it is slower. We have plotted the age of the Universe and the big rip time as a function of n in Figure 3 to show their different evolutions.

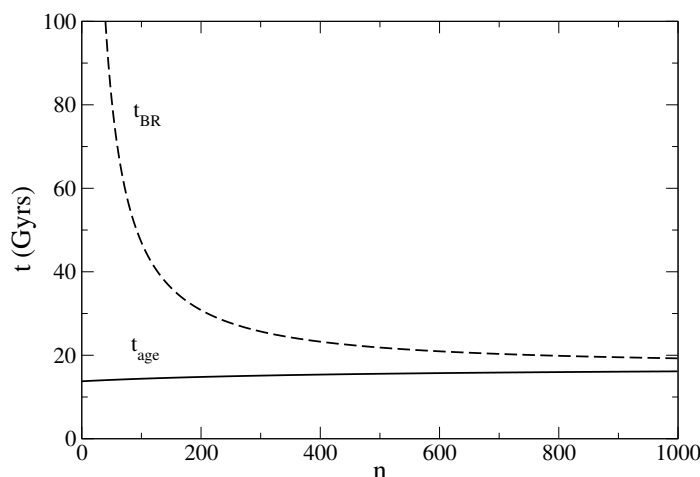


Figure 3. Age of the Universe t_{age} and big rip time t_{BR} as a function of n .

Using Equations (38) and (39), the EoS parameter $w = P/\epsilon$ can be expressed in terms of the scale factor as

$$w(a) = \frac{-(1 - \Omega_{m,0})e^{1+1/B}a^3 \left(-1 - \frac{1}{B} - 3 \ln a\right)^n}{\Omega_{m,0}\Gamma\left(n + 1, -1 - \frac{1}{B}\right) + (1 - \Omega_{m,0})\Gamma\left(n + 1, -1 - \frac{1}{B} - 3 \ln a\right)}. \quad (82)$$

For $a = 1$, we obtain

$$w_0 = -\frac{(1 - \Omega_{m,0})e^{1+1/B} \left(-1 - \frac{1}{B}\right)^n}{\Gamma\left(n + 1, -1 - \frac{1}{B}\right)}. \quad (83)$$

For the Λ CDM ($n = 0$) we recover the well-known value $w_0 = -(1 - \Omega_{m,0}) = -0.691$. We obtain $w_0 = -0.693$ for $n = 1$, $w_0 = -0.696$ for $n = 2$, $w_0 = -0.698$ for $n = 3$, $w_0 = -0.701$ for $n = 4$, $w_0 = -0.715$ for $n = 10$, $w_0 = -0.935$ for $n = 100$, and $w_0 = -3.12$ for $n = 1000$. For $n > 3$ we are out of the error bars (typically 1% for the value of w_0) so these models should be rejected. The behavior of the EoS parameter $w(a)$ as a function of the scale factor a is plotted in Figure 4. The GLDF behaves as a superposition of two non-interacting fluids (i.e., DM and DE) whose total pressure and total energy density are given by the sums

$$P = P_m + P_{de}, \quad \epsilon = \epsilon_m + \epsilon_{de}. \tag{84}$$

Their EoS parameters are

$$w_m = \frac{P_m}{\epsilon_m} = 0, \quad w_{de} = \frac{P_{de}}{\epsilon_{de}} = -\frac{e^{1+1/B} a^3 \left(-1 - \frac{1}{B} - 3 \ln a\right)^n}{\Gamma\left(n + 1, -1 - \frac{1}{B} - 3 \ln a\right)}. \tag{85}$$

In a flat Universe, the deceleration parameter $q = -\ddot{a}a/\dot{a}^2 = -\dot{H}/H^2 - 1$ is related to the EoS parameter by

$$q = \frac{1 + 3w}{2}. \tag{86}$$

The Universe is undergoing a decelerating expansion if $q > 0$ (i.e., $w > -1/3$) and an accelerating expansion if $q < 0$ (i.e., $w < -1/3$). In Figure 5, we show the behavior of $q(a)$ as a function of the scale factor for different values of n .

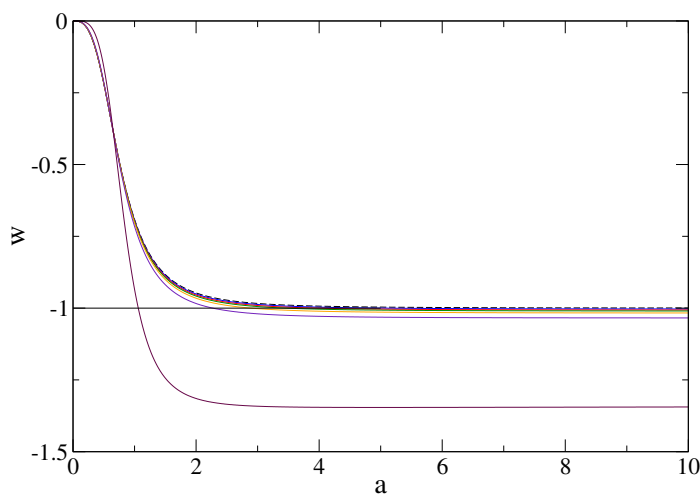


Figure 4. EoS parameter w as a function the scale factor a for $\Omega_{m,0} = 0.309$, $B = 3.53 \times 10^{-3}$ and $n = 0, 1, 2, 3, 5, 10, 100$.

From Equation (39), the transition scale factor a_t , corresponding to $\epsilon_m = \epsilon_{de}$ is obtained by solving the transcendental equation

$$\Gamma\left(n + 1, -1 - \frac{1}{B} - 3 \ln a_t\right) = \frac{\Omega_{m,0}}{1 - \Omega_{m,0}} \Gamma\left(n + 1, -1 - \frac{1}{B}\right). \tag{87}$$

Another parameter to study is the squared speed of sound c_s^2 which is a key ingredient to investigate the stability of any model. In particular, the sign of c_s^2 plays a crucial role in determining classical stability. It is defined by

$$c_s^2 = \frac{dP}{d\epsilon} c^2 = \frac{dP/d\rho_m}{d\epsilon/d\rho_m} c^2. \tag{88}$$

Differentiating Equations (1) and (13) with $A_i = A_n \delta_{i,n}$, we obtain

$$\frac{c_s^2}{c^2} = \frac{n \ln^{n-1} \left(\frac{\rho_m}{\rho_p} \right)}{\frac{\rho_m c^2}{A_n} - n \frac{\rho_m}{\rho_p} \Gamma \left[n, \ln \left(\frac{\rho_m}{\rho_p} \right) \right]} \tag{89}$$

To obtain this expression, we have used the identities

$$\Gamma(n + 1, x) = n\Gamma(n, x) + x^n e^{-x} \tag{90}$$

and

$$\frac{\partial \Gamma}{\partial x}(n + 1, x) = -x^n e^{-x}. \tag{91}$$

In Figure 6, we plot the squared speed of sound c_s^2/c^2 as a function of the scale factor for different values of n . The causality and classical stability conditions are satisfied if the speed of sound varies in the range $0 \leq c_s^2/c^2 \leq 1$. One sees from Figure 6 that, in fact, there are regions where the causality and classical stability conditions are satisfied but the extent of these regions decreases as n increases ⁷.

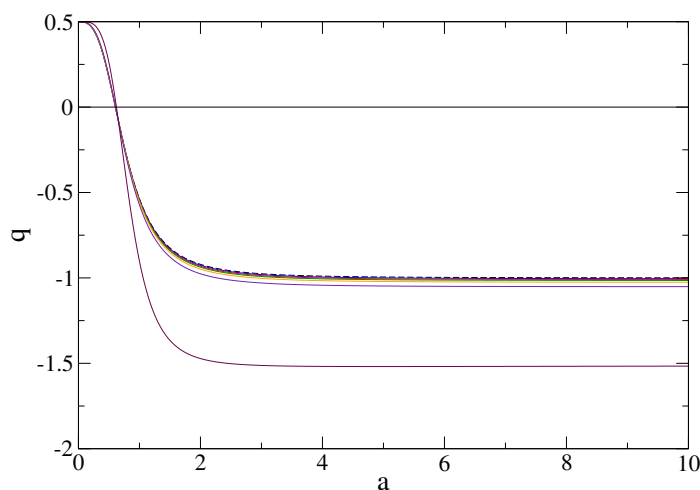


Figure 5. Deceleration parameter q as a function of the scale factor a for $\Omega_{m,0} = 0.309$, $B = 3.53 \times 10^{-3}$ and $n = 0, 1, 2, 3, 5, 10, 100$.

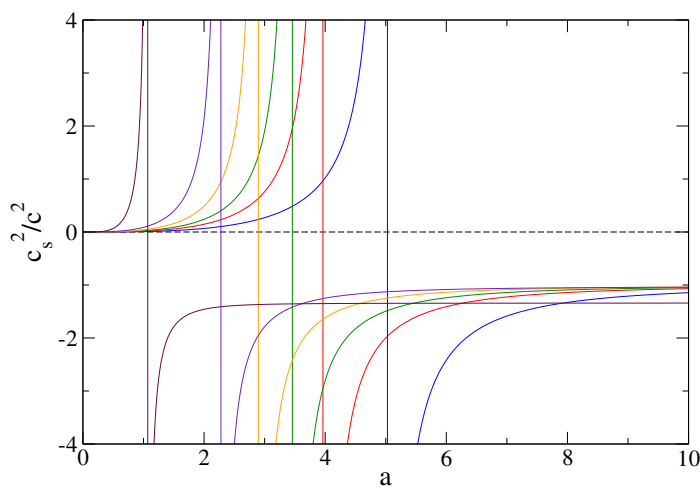


Figure 6. Normalized squared speed of sound c_s^2/c^2 as a function of the scale factor a for $\Omega_{m,0} = 0.309$, $B = 3.53 \times 10^{-3}$ and $n = 0, 1, 2, 3, 5, 10, 100$. It diverges and becomes negative when the Universe becomes phantom.

6. Conclusions

In this work, we have proposed a new class of cosmological unified dark sector models “Generalized Logotropic Models”. These models are a generalization of the logotropic model [30] by considering the pressure P as a sum of higher logarithmic terms of the rest-mass density ρ_m . The pressure can naturally take negative values in these cosmological models. In this scenario, the Universe is filled with a single fluid without the need for a cosmological constant. Our generalized model depends on a set of free parameters A_i with $i = 1, 2, \dots, N$. In particular, we have considered a special class of generalized logotropic models where $A_i = A_n \delta_{in}$, which depends on two free parameters A_n and n . The usual logotropic model [30] corresponds to $n = 1$ and A_1 . We have also presented the model with $N = 2$, which contains the first two terms A_1 and A_2 of the series. We have highlighted the most relevant properties of these generalized logotropic models. To fix bounds on the free parameters of our models, we employed the best fit of the parameters $\Omega_{m,0}$ and B obtained from the cosmological analysis carried on the original logotropic model (i.e., $n = 1$) [40]. After fixing the free parameters, we investigated the cosmological behavior of the generalized logotropic models by focusing on the evolution of the DE density, scale factor, EoS parameter, deceleration parameter and squared speed of sound. We showed the asymptotic behavior of these models and noticed three distinct ways of evolution depending on the value of n . In all the analyzed cases, we established that generalized logotropic models lead to realistic cosmological models in which the dark sector is represented by a unique fluid. The deviation of the generalized models from the standard Λ CDM model depends on the value of the parameter n . At later times, higher values of n lead to higher deviations from Λ CDM. This implies that the generalized logotropic models can be used as realistic background cosmological models to describe our Universe with a free parameter n . We estimated that only models with $n \leq 3$ are consistent with the observations. To find out the most suitable values of n , it will be necessary to perform a fitting procedure by using, for instance, the Monte Carlo method and a detailed comparison with cosmological data such as SN, BAO, and CMB surveys. We expect to perform this analysis in future works.

A further interesting generalization of the logotropic model is to consider a single fluid described by the EoS

$$P = A \ln^\alpha \left(\frac{\rho_m}{\rho_P} \right), \tag{92}$$

where A is a real number given by

$$A = - \frac{(1 - \Omega_{m,0}) \epsilon_0 e^{1+1/B}}{\Gamma \left(\alpha + 1, -1 - \frac{1}{B} \right)}, \tag{93}$$

and α is a real positive parameter that can be constrained by the cosmological data. There are two ways to recover the Λ CDM, either by taking $\alpha = 0$ or $B = 0$ which makes the model rich and particularly more appealing in describing DE especially for $0 < \alpha < 1$. Such a model interpolates between the Λ CDM for values of α close to zero and to the usual logotropic model for values of α close to one.

In summary, single fluids with generalized logotropic EoS may have interesting cosmological features and, thus, they represent a good candidate to describe the DE sector. The investigation and analysis of these models will be carried out in detail in future works.

Finally, we would like to mention that the logotropic model and the generalization presented in this work are not free of intrinsic problems, as all the cosmological models known in the literature. In fact, the speed of sound in logotropic models has the unpleasant property of increasing with the scale factor, leading, like for the Chaplygin gas model, to oscillations in the mass power-spectrum that are not detected in observations at the cosmological level [51]. However, there are several possibilities to solve this problem by

considering additional effects such as non-linear and non-adiabatic perturbations, or higher order derivatives in K-essence Lagrangians associated with braneworld models, among others (see the discussion in Section XVI.G of [46]). These modifications could solve the problems in the theory of perturbations for structure formation (e.g., by reducing the speed of sound) without affecting the evolution of the cosmological background. In any case, UDM models constitute a subject of intensive research as possible alternative scenarios to the popular and generally accepted Λ CDM model. Our paper provides a class of models exhibiting a transition between a normal behavior and a phantom behavior governed by a single equation of state. In addition, depending on the value of the parameter n , we can have different types of late evolution: no singularity ($n = 0$), little rip ($n \leq 2$), big rip ($n > 2$). It is very interesting to note that all these models are consistent with the Λ CDM model up to the present time but will differ in the future. Therefore, it is possible to construct models that agree with the observations but that deviate from each other at late times. A virtue of our model is to show that it is very difficult to predict the future evolution of the Universe based on present observations.

Author Contributions: Formal analysis, H.B., P.-H.C. and H.Q.; investigation, H.B., P.-H.C. and H.Q.; writing—original draft preparation, H.B., P.-H.C. and H.Q.; writing—review and editing, H.B., P.-H.C. and H.Q. All authors have read and agreed to the published version of the manuscript.

Funding: The work of H.Q. was partially supported by UNAM-DGAPA-PAPIIT, Grant No. 114520, and Conacyt-Mexico, Grant No. A1-S-31269.

Institutional Review Board Statement: Not applicable.

Informed Consent Statement: Not applicable.

Data Availability Statement: Not applicable.

Acknowledgments: We would like to thank O. Luongo for helpful comments. HBB gratefully acknowledges the financial support from University of Sharjah (grant number V.C.R.G./R.438/2020).

Conflicts of Interest: The authors declare no conflict of interest.

Appendix A. Asymptotic Equation of State

In this Appendix, we establish the asymptotic EoS $P(\epsilon)$ of the GLDF and make the connection with the MCG model [19,26–28].

For $a \rightarrow +\infty$, using Equations (19) and (28), we find that the energy density evolves with the scale factor as

$$\epsilon \sim |A_N| \left(1 + \frac{1}{B} + 3 \ln a \right)^N. \tag{A1}$$

Let us determine the corresponding asymptotic EoS from the energy conservation Equation (10) which can be rewritten as

$$\frac{d\epsilon}{da} + \frac{3}{a}(\epsilon + P) = 0. \tag{A2}$$

From Equations (A1) and (A2), we obtain

$$\begin{aligned} P &= -\epsilon - \frac{a}{3} \frac{d\epsilon}{da} \\ &= -\epsilon - N|A_N| \left(1 + \frac{1}{B} + 3 \ln a \right)^{N-1} \\ &= -\epsilon - N|A_N| \left(\frac{\epsilon}{|A_N|} \right)^{(N-1)/N} \\ &= -\epsilon \left[1 + N \left(\frac{|A_N|}{\epsilon} \right)^{1/N} \right]. \end{aligned} \tag{A3}$$

Therefore, the asymptotic EoS of the GLDF reads

$$P = -\epsilon - N|A_N|^{1/N}\epsilon^{1-1/N}. \tag{A4}$$

This is a particular case of the generalized polytropic EoS (or MCG model) [19,26–28]

$$P = \alpha\epsilon + K\left(\frac{\epsilon}{c^2}\right)^\gamma \tag{A5}$$

corresponding to $\alpha = -1$, $K = -N(|A_N|c^2)^{1/N}$ and $\gamma = 1 - 1/N$. Therefore, the GLDF is asymptotically equivalent to the MCG with $\alpha = -1$. Since $w = P/\epsilon < -1$, the EoS (A4) leads to a phantom behavior in agreement with the results of Section 5. For $N = 1$, the EoS (A4) reduces to

$$P = -\epsilon - A. \tag{A6}$$

For $N = 2$, it reduces to

$$P = -\epsilon - 2\sqrt{|A_2|}\epsilon^{1/2}. \tag{A7}$$

Let us check that we recover the asymptotic EoS (A4) directly from the generalized logotropic EoS defined by Equations (27) and (28). For $a \rightarrow +\infty$, we have

$$P \simeq A_N x^N + A_{N-1} x^{N-1} + \dots, \tag{A8}$$

$$\epsilon \simeq -A_N x^N - A_N N x^{N-1} - A_{N-1} x^{N-1} + \dots, \tag{A9}$$

where

$$x \equiv -1 - \frac{1}{B} - 3 \ln a \rightarrow -\infty. \tag{A10}$$

We stress that it is necessary to account for the first order correction to the leading term x^N in Equations (A8) and (A9). From

$$P \simeq A_N x^N \left(1 + \frac{A_{N-1}}{A_N} \frac{1}{x}\right), \tag{A11}$$

$$\epsilon \simeq -A_N x^N \left(1 + N \frac{1}{x} + \frac{A_{N-1}}{A_N} \frac{1}{x}\right), \tag{A12}$$

we obtain

$$\begin{aligned} \frac{P}{\epsilon} &\simeq -\left(1 + \frac{A_{N-1}}{A_N} \frac{1}{x}\right) \left(1 - N \frac{1}{x} - \frac{A_{N-1}}{A_N} \frac{1}{x}\right) \\ &\simeq -\left(1 - \frac{N}{x}\right) \\ &= -\left[1 + N \left(\frac{|A_N|}{\epsilon}\right)^{1/N}\right], \end{aligned} \tag{A13}$$

which returns Equation (A3).

Appendix B. The Two-Fluid Model

In this Appendix, we determine the two-fluid model corresponding to the GLDF with $A_i = A_n \delta_{i,n}$. In particular, we establish the EoS of the DE in the two-fluid model.

The GLDF is a one-fluid model (i.e., a UDM model) unifying DM and DE. The pressure and the energy density are given by

$$P = A_n \ln^n \left(\frac{\rho_m}{\rho_P}\right), \tag{A14}$$

$$\epsilon = \rho_m c^2 - A_n \frac{\rho_m}{\rho_P} \Gamma \left[n + 1, \ln \left(\frac{\rho_m}{\rho_P} \right) \right] = \rho_m c^2 + u = \epsilon_m + \epsilon_{de}. \tag{A15}$$

Concerning the evolution of the homogeneous background, this one-fluid model is equivalent ⁸ to a two-fluid model made of pressureless DM with an EoS $P_m = 0$ giving $\epsilon_m = \Omega_{m,0} \epsilon_0 / a^3$ and DE with an EoS $P_{de}(\epsilon_{de})$ giving $\epsilon_{de} = u(a)$. Noting that $P = P_m + P_{de} = P_{de}$, the EoS $P_{de}(\epsilon_{de})$ of DE is determined in parametric form by the equations

$$P_{de} = A_n \ln^n \left(\frac{\rho_m}{\rho_P} \right), \tag{A16}$$

$$\epsilon_{de} = -A_n \frac{\rho_m}{\rho_P} \Gamma \left[n + 1, \ln \left(\frac{\rho_m}{\rho_P} \right) \right]. \tag{A17}$$

Eliminating ρ_m between these two expressions we obtain the EoS of DE under the reversed form $\epsilon_{de}(P_{de})$ as

$$\epsilon_{de} = -A_n e^{\mp \left| \frac{P_{de}}{A_n} \right|^{1/n}} \Gamma \left[n + 1, \mp \left| \frac{P_{de}}{A_n} \right|^{1/n} \right], \tag{A18}$$

where the upper sign corresponds to the most relevant case $\rho_m < \rho_P$ and the lower sign corresponds to $\rho_m > \rho_P$.

Let us check that the two-fluid model returns the results of the one-fluid model for the homogeneous background. The evolution $\epsilon_{de}(a)$ of the DE density with the scale factor can be obtained from the energy conservation equation

$$\frac{d\epsilon_{de}}{da} + \frac{3}{a}(\epsilon_{de} + P_{de}) = 0 \quad \Leftrightarrow \quad \int \frac{d\epsilon_{de}}{\epsilon_{de} + P_{de}} = -3 \ln a \tag{A19}$$

with the EoS $P_{de}(\epsilon_{de})$ defined by Equations (A16) and (A17). At this stage, ρ_m is just a dummy variable. It is easy to establish that

$$\epsilon'_{de}(\rho_m) = -A_n n \frac{\rho_P}{\rho_m^2} \Gamma \left[n, \ln \left(\frac{\rho_m}{\rho_P} \right) \right] \tag{A20}$$

and

$$P_{de}(\rho_m) + \epsilon_{de}(\rho_m) = -A_n n \frac{\rho_P}{\rho_m} \Gamma \left[n, \ln \left(\frac{\rho_m}{\rho_P} \right) \right]. \tag{A21}$$

Therefore, we have the identity

$$P_{de}(\rho_m) + \epsilon_{de}(\rho_m) = \rho_m \epsilon'_{de}(\rho_m), \tag{A22}$$

and the energy conservation Equation (A19) becomes

$$\frac{d\rho_m}{da} + \frac{3}{a} \rho_m = 0 \quad \Leftrightarrow \quad \int \frac{d\rho_m}{\rho_m} = -3 \ln a, \tag{A23}$$

implying that $\rho_m \propto a^{-3}$. This leads to results consistent with those of Section 4. However, we cannot establish that ρ_m is the rest-mass (or DM) density (they could differ by a multiplicative constant). This implies that we cannot determine A_n in the two-fluid model contrary to the one-fluid model. More explicit results are given below.

Appendix B.1. The Case $n = 1$

For $n = 1$, Equation (A18) reduces to the affine EoS

$$P_{de} = -\epsilon_{de} - A \tag{A24}$$

with $A > 0$. This is the EoS of DE corresponding to the original logotropic gas [40]. It coincides with the asymptotic EoS (A6) of the LDF seen as a one-fluid (UDM) model. The affine EoS (A24) was first introduced and studied in [28].

Let us check that the two-fluid model returns the results of the one-fluid model. Integrating the energy conservation Equation (A19) for DE with the EoS (A24) we obtain

$$\epsilon_{de} = 3A \ln\left(\frac{a}{a_*}\right), \tag{A25}$$

where a_* is a constant of integration. If we add the contribution of pressureless DM, we find that the total energy density is given by

$$\epsilon = \frac{\Omega_{m,0}\epsilon_0}{a^3} + 3A \ln\left(\frac{a}{a_*}\right). \tag{A26}$$

Using the condition (at $a = 1$)

$$\epsilon_0(1 - \Omega_{m,0}) = -3A \ln a_*, \tag{A27}$$

we can rewrite Equation (A26) under the form

$$\epsilon = \frac{\Omega_{m,0}\epsilon_0}{a^3} + 3A \ln a + \epsilon_0(1 - \Omega_{m,0}). \tag{A28}$$

This expression is consistent with Equation (53) of the one-fluid model if we set $A = B\epsilon_0(1 - \Omega_{m,0})$. However, the two-fluid model does *not* determine the value of the constant A , contrary to the one-fluid model. Indeed, the Planck scale ρ_P does not occur in Equation (A24), unlike Equation (46). This is a huge advantage of the one-fluid model with respect to the two-fluid model [30].

Appendix B.2. The Case $n = 2$

For $n = 2$, Equation (A18) reduces to

$$\epsilon_{de} = -2A_2 \left(1 \mp \sqrt{\frac{P_{de}}{A_2} + \frac{P_{de}}{2A_2}} \right) \tag{A29}$$

with $A_2 < 0$. This yields a second degree equation for $\sqrt{P_{de}/A_2}$ of the form

$$\frac{P_{de}}{A_2} \mp 2\sqrt{\frac{P_{de}}{A_2}} + 2 + \frac{\epsilon_{de}}{A_2} = 0. \tag{A30}$$

When $\rho_m > \rho_P$, Equation (A30) with the lower sign has just one solution

$$\sqrt{-\frac{P_{de}}{|A_2|}} = -1 + \sqrt{\frac{\epsilon_{de}}{|A_2|} - 1}. \tag{A31}$$

As ρ_m decreases from $+\infty$ to ρ_P , the DE density ϵ_{de} decreases from $+\infty$ to $2|A_2|$ and the pressure P_{de} increases from $-\infty$ to 0 (see Section 4.4). This leads to the EoS

$$P_{de} = -|A_2| \left(-1 + \sqrt{\frac{\epsilon_{de}}{|A_2|} - 1} \right)^2 \tag{A32}$$

or, equivalently,

$$P_{de} = -\epsilon_{de} + 2|A_2|\sqrt{\frac{\epsilon_{de}}{|A_2|} - 1}, \tag{A33}$$

which is valid for $\epsilon_{de} \geq 2|A_2|$. For $\epsilon_{de} \rightarrow +\infty$, Equation (A33) reduces to

$$P_{de} \simeq -\epsilon_{de} + 2|A_2|^{1/2}\sqrt{\epsilon_{de}}. \tag{A34}$$

When $\rho_m < \rho_P$, the solutions of Equation (A30) with the upper sign are

$$\sqrt{-\frac{P_{de}}{|A_2|}} = 1 \pm \sqrt{\frac{\epsilon_{de}}{|A_2|} - 1}. \tag{A35}$$

As ρ_m goes from ρ_P to 0, the DE density ϵ_{de} first decreases from $2|A_2|$ to $|A_2|$ then increases to $+\infty$ while the pressure P_{de} decreases from 0 to $-\infty$ (see Section 4.4). Equation (A30) has two solutions for $|A_2| \leq \epsilon_{de} \leq 2|A_2|$, one solution (with the upper sign) for $\epsilon_{de} \geq 2|A_2|$ and no solution for $\epsilon_{de} \leq |A_2|$. This leads to the EoS

$$P_{de} = -|A_2|\left(1 \pm \sqrt{\frac{\epsilon_{de}}{|A_2|} - 1}\right)^2 \tag{A36}$$

or, equivalently,

$$P_{de} = -\epsilon_{de} \mp 2|A_2|\sqrt{\frac{\epsilon_{de}}{|A_2|} - 1}, \tag{A37}$$

which is valid with the two signs for $|A_2| \leq \epsilon_{de} \leq 2|A_2|$ and with the upper sign for $\epsilon_{de} \geq 2|A_2|$. This is the EoS of DE corresponding to the GLDF in the case $n = 2$. For $\epsilon_{de} \rightarrow +\infty$, Equation (A37) reduces to

$$P_{de} \simeq -\epsilon_{de} - 2|A_2|^{1/2}\sqrt{\epsilon_{de}}, \tag{A38}$$

which coincides with the asymptotic EoS (A7) of the GLDF seen as a one-fluid (UDM) model.

Let us check that the two-fluid model returns the results of the one-fluid model. Integrating the energy conservation Equation (A19) for DE with the EoS (A33) or (A37) we obtain

$$\frac{\epsilon_{de}}{|A_2|} = 1 + 9 \ln^2\left(\frac{a}{a_*}\right), \tag{A39}$$

where a_* is a constant of integration. If we add the contribution of pressureless DM, we find that the total energy density is given by

$$\epsilon = \frac{\Omega_{m,0}\epsilon_0}{a^3} + |A_2|\left[1 + 9 \ln^2\left(\frac{a}{a_*}\right)\right]. \tag{A40}$$

Using the condition (at $a = 1$)

$$\epsilon_0(1 - \Omega_{m,0}) = |A_2|\left(1 + 9 \ln^2 a_*\right), \tag{A41}$$

we can rewrite Equation (A40) under the form

$$\epsilon = \frac{\Omega_{m,0}\epsilon_0}{a^3} + \epsilon_0(1 - \Omega_{m,0})\left[1 + \frac{9|A_2|\ln^2 a}{\epsilon_0(1 - \Omega_{m,0})} + \frac{6|A_2|\ln a}{\epsilon_0(1 - \Omega_{m,0})}\sqrt{\frac{\epsilon_0(1 - \Omega_{m,0})}{|A_2|} - 1}\right]. \tag{A42}$$

This expression is consistent with Equation (61) of the one-fluid model if we set $|A_2|/[\epsilon_0(1 - \Omega_{m,0})] = B^2/(1 + B^2)$. However, the two-fluid model does *not* determine the value of the constant A_2 , contrary to the one-fluid model. This is a huge advantage of the one-fluid model with respect to the two-fluid model [30].

Appendix C. Present Proportions of Dark Matter and Dark Energy

In this Appendix we recall the argument of [35] leading to a prediction of the present proportions of DM and DE in the universe and take into account the presence of baryons (see also [44]).

The original logotropic model [30,31,35,40] is based on the EoS

$$P = A \ln\left(\frac{\rho_{dm}}{\rho_P}\right), \tag{A43}$$

where ρ_{dm} is the rest-mass density of the LDF, A is a new fundamental constant of physics (superseding the cosmological constant Λ) and ρ_P is the Planck density. This EoS provides a unification of DM and DE. It is very interesting that the Planck density appears in this EoS in order to make the variable in the logarithm dimensionless. This implies that quantum effects play a certain role in the late universe where the logotropic model applies. The rest-mass density evolves as (see Equation (21))

$$\rho_{dm} = \frac{\Omega_{dm,0}\epsilon_0/c^2}{a^3}, \tag{A44}$$

and it plays the role of DM. As a result $\Omega_{dm,0}$ is interpreted as the present proportion of DM in the universe. The energy density of the LDF is (see Equation (47))

$$\epsilon_{df} = \rho_{dm}c^2 - A \left[1 + \ln\left(\frac{\rho_{dm}}{\rho_P}\right) \right] = \epsilon_{dm} + \epsilon_{de}, \tag{A45}$$

where the first term (rest-mass) is interpreted as DM and the second term (internal energy) as DE. We must also include the contribution of baryons which form a pressureless gas ($P_b = 0$). Their energy density evolves as

$$\epsilon_b = \frac{\Omega_{b,0}\epsilon_0}{a^3}, \tag{A46}$$

where $\Omega_{b,0}$ is the present proportion of baryons in the universe. The total energy density is therefore

$$\epsilon = \rho_{dm}c^2 - A \left[1 + \ln\left(\frac{\rho_{dm}}{\rho_P}\right) \right] + \epsilon_b. \tag{A47}$$

Substituting Equation (A44) into Equation (A47), we obtain

$$\epsilon = \frac{\Omega_{dm,0}\epsilon_0}{a^3} - A \left[1 + \ln\left(\frac{\Omega_{dm,0}\epsilon_0}{\rho_P c^2 a^3}\right) \right] + \frac{\Omega_{b,0}\epsilon_0}{a^3}. \tag{A48}$$

Applying this relation at the present time ($a = 1$) and introducing the present proportion of DE in the universe $\Omega_{de,0} = 1 - \Omega_{dm,0} - \Omega_{b,0}$ we get

$$A = \frac{\Omega_{de,0}\epsilon_0}{\ln\left(\frac{\rho_P c^2}{\Omega_{dm,0}\epsilon_0}\right) - 1}. \tag{A49}$$

Introducing the present DE density $\rho_\Lambda \equiv \Omega_{de,0}\epsilon_0/c^2$, we can rewrite the foregoing equation as

$$A = \frac{\rho_\Lambda c^2}{\ln\left(\frac{\rho_P}{\rho_\Lambda}\right) + \ln\left(\frac{\Omega_{de,0}}{1 - \Omega_{de,0} - \Omega_{b,0}}\right) - 1}. \tag{A50}$$

We now postulate that [35,44]

$$A = \frac{\rho_\Lambda c^2}{\ln\left(\frac{\rho_P}{\rho_\Lambda}\right)} \tag{A51}$$

or, equivalently, that $B = 1/\ln(\rho_P/\rho_\Lambda)$, i.e., $\rho_P/\rho_\Lambda = e^{1/B}$. This implies

$$\frac{\Omega_{de,0}}{1 - \Omega_{de,0} - \Omega_{b,0}} = e, \tag{A52}$$

determining the present proportions of DM and DE [35,44]

$$\Omega_{de,0}^{th} = \frac{e}{1+e}(1 - \Omega_{b,0}), \quad \Omega_{dm,0}^{th} = \frac{1}{1+e}(1 - \Omega_{b,0}). \tag{A53}$$

If we neglect baryonic matter $\Omega_{b,0} = 0$ we obtain the pure numbers $\Omega_{de,0}^{th} = \frac{e}{1+e} = 0.731059\dots$ and $\Omega_{dm,0}^{th} = \frac{1}{1+e} = 0.268941\dots$ which give the correct proportions 70% and 25% of DE and DM [35]. If we take baryonic matter into account and use the measured value of $\Omega_{b,0} = 0.0486 \pm 0.0010$, we obtain $\Omega_{de,0}^{th} = 0.6955 \pm 0.0007$ and $\Omega_{dm,0}^{th} = 0.2559 \pm 0.0003$ which are very close to the observed values $\Omega_{de,0} = 0.6911 \pm 0.0062$ and $\Omega_{dm,0} = 0.2589 \pm 0.0057$ within the error bars [44]. The present ratio of DE and DM [see Equation (A52)] is predicted to be equal to the Euler number: $\Omega_{de,0}^{th}/\Omega_{dm,0}^{th} = e = 2.71828\dots$ [44] in good agreement with the empirical value $\Omega_{de,0}/\Omega_{dm,0} = 2.669 \pm 0.08$. The postulate from Equation (A51) means that the fundamental constant A is equal to the present DE energy density (more precisely $\rho_\Lambda c^2 / \ln(\rho_P/\rho_\Lambda)$). This can be viewed as a strong cosmic coincidence [35,44] giving to our epoch a central place in the history of the universe.

Notes

- 1 We have assumed that n is an integer. However, it can be shown that this asymptotic behavior remains valid when n is a real number.
- 2 The notation ρ_m stands either for pressureless DM density or for rest-mass density.
- 3 More precisely, our model has the same number of parameters as the Λ CDM model. In principle, these parameters should be determined from the observations for each value of n . For convenience, we shall use the values of $\Omega_{m,0}$ and ϵ_0 obtained from the Λ CDM model taken as a reference. In that case, there is no undetermined parameter in our model except, of course, the value of n .
- 4 We can note that Equation (62) is a second degree equation in $\ln(\rho_m/\rho_P)$.
- 5 We recall that the logotropic model is not aimed at describing the early inflation.
- 6 Some concerns could arise regarding the procedure we use to find out the constraint on the parameter n . Indeed, we first fix the values of $\Omega_{m,0}$ and H_0 by following the Λ CDM model, and then, by evaluating the age of the Universe in the logotropic model, we conclude that models with $n > 3$ are excluded. A better procedure would be to evaluate all the parameters of the logotropic model directly from observational data to determine the age of the Universe. However, this procedure would imply determining the values of the observables in terms of n , which is a long and arduous process. This, however, would not change the main conclusion regarding the constraint on n because the predicted values of the observables are very similar in both models (for not too large values of n). Therefore, we can use the Λ CDM values as a reference to determine the values of the observables in the logotropic model (see footnote 3).
- 7 The speed of sound is real in the normal regime $d\epsilon/d\rho_m > 0$ and imaginary in the phantom regime $d\epsilon/d\rho_m < 0$. It becomes infinite (before becoming imaginary) when we enter into the phantom regime, i.e., when $d\epsilon/d\rho_m = 0$.
- 8 The equivalence between the one-fluid model and the two-fluid model is lost when we consider the theory of perturbations and the formation of structures.

References

1. Riess, A.G.; Filippenko, A.V.; Challis, P.; Clocchiatti, A.; Diercks, A.; Garnavich, P.M.; Gilliland, R.L.; Hogan, C.J.; Jha, S.; Tonry, J. Observational evidence from supernovae for an accelerating universe and a cosmological constant. *Astron. J.* **1998**, *116*, 1009. [[CrossRef](#)]
2. Perlmutter, S.; Aldering, G.; Goldhaber, G.; Knop, R.A.; Nugent, P.; Castro, P.G.; Deustua, S.; Fabbro, S.; Goobar, A.; Groom, D.E.; et al. Supernova Cosmology Project. Measurements of Ω and Λ from 42 high-redshift supernovae. *Astrophys. J.* **1999**, *517*, 565. [[CrossRef](#)]
3. Spergel, D.N.; Verde, L.; Peiris, H.V.; Komatsu, E.; Nolta, M.R.; Bennett, C.L.; Halpern, M.; Hinshaw, G.; Jarosik, N.; Wright, E.L.; et al. First-year Wilkinson Microwave Anisotropy Probe (WMAP)* observations: Determination of cosmological parameters. *Astrophys. J. Suppl. Ser.* **2003**, *148*, 175. [[CrossRef](#)]
4. Tegmark, M.; Strauss, M.A.; Blanton, M.R.; Abazajian, K.; Dodelson, S.; Sandvik, H.; York, D.G. Cosmological parameters from SDSS and WMAP. *Phys. Rev. D* **2004**, *69*, 103501. [[CrossRef](#)]
5. Ade, P.A.R.; Aghanim, N.; Armitage-Caplan, C.; Arnau, M.; Ashdown, M.; Atrio-Barandela, F.; Aumont, J.; Baccigalupi, C.; Banday, A.J.; Meinhold, P.R.; et al. Planck 2013 results. XVI. Cosmological parameters. *Astron. Astrophys.* **2014**, *571*, A16.
6. Sahni, V.; Starobinsky, A.A. The case for a positive cosmological Λ -term. *Int. J. Modern Phys. D* **2000**, *9*, 373–443. [[CrossRef](#)]
7. Amendola, L.; Kunz, M.; Motta, M.; Saltas, I.D.; Sawicki, I. Observables and unobservables in dark energy cosmologies. *Phys. Rev. D* **2013**, *87*, 023501. [[CrossRef](#)]
8. Weinberg, S. The cosmological constant problem. *Rev. Mod. Phys.* **1989**, *61*, 1. [[CrossRef](#)]
9. Padmanabhan, T. Cosmological Constant—The Weight of the Vacuum. *Phys. Rep.* **2003**, *380*, 235. [[CrossRef](#)]
10. Steinhardt, P. *Critical Problems in Physics*; Fitch, V.L., Marlow, D.R., Eds.; Princeton University Press: Princeton, NJ, USA, 1997.
11. Zlatev, I.; Wang, L.; Steinhardt, P.J. Quintessence, cosmic coincidence, and the cosmological constant. *Phys. Rev. Lett.* **1999**, *82*, 896. [[CrossRef](#)]
12. Moore, B.; Quinn, T.; Governato, F.; Stadel, J.; Lake, G. Cold collapse and the core catastrophe. *Mon. Not. R. Astron. Soc.* **1999**, *310*, 1147–1152. [[CrossRef](#)]
13. Kauffmann, G.; White, S.D.M.; Guiderdoni, B. The formation and evolution of galaxies within merging dark matter haloes. *Mon. Not. R. Astron. Soc.* **1993**, *264*, 201–218. [[CrossRef](#)]
14. Klypin, A.; Kravtsov, A.V.; Valenzuela, O. Where are the missing galactic satellites? *Astrophys. J.* **1999**, *522*, 82. [[CrossRef](#)]
15. Kamionkowski, M.; Liddle, A.R. The dearth of halo dwarf galaxies: Is there power on short scales? *Phys. Rev. Lett.* **2000**, *84*, 4525. [[CrossRef](#)]
16. Boylan-Kolchin, M.; Bullock, J.S.; Kaplinghat, M. Too big to fail? The puzzling darkness of massive Milky Way subhaloes. *Mon. Not. R. Astron. Soc. Lett.* **2011**, *415*, L40–L44. [[CrossRef](#)]
17. Bullock, J.S.; Boylan-Kolchin, M. Small-Scale Challenges to the Λ CDM Paradigm. *Ann. Rev. Astron. Astrophys.* **2017**, *55*, 343. [[CrossRef](#)]
18. Kamenshchik, A.; Moschella, U.; Pasquier, V. An alternative to quintessence. *Phys. Lett. B* **2001**, *511*, 265–268. [[CrossRef](#)]
19. Benaoum, H.B. Accelerated Universe from Modified Chaplygin Gas and Tachyonic Fluid. *Universe* **2022**, *8*, 340. [[CrossRef](#)]
20. Bento, M.C.; Bertolami, O.; Sen, A.A. Generalized Chaplygin gas, accelerated expansion, and dark-energy-matter unification. *Phys. Rev. D* **2002**, *66*, 043507. [[CrossRef](#)]
21. Gorini, V.; Kamenshchik, A.; Moschella, U. Can the Chaplygin gas be a plausible model for dark energy? *Phys. Rev. D* **2003**, *67*, 063509. [[CrossRef](#)]
22. Bento, M.C.; Bertolami, O.; Sen, A.A. Revival of the unified dark energy–dark matter model? *Phys. Rev. D* **2004**, *70*, 083519. [[CrossRef](#)]
23. Debnath, U.; Banerjee, A.; Chakraborty, S. Role of modified Chaplygin gas in accelerated universe. *Class. Quantum Grav.* **2004**, *21*, 5609. [[CrossRef](#)]
24. Benaoum, H.B. Modified Chaplygin Gas Cosmology. *Adv. High Energy Phys.* **2012**, *2012*, 357802. [[CrossRef](#)]
25. Benaoum, H.B. Modified Chaplygin gas cosmology with bulk viscosity. *Int. J. Mod. Phys. D* **2014**, *23*, 1450082. [[CrossRef](#)]
26. Chavanis, P.H. Models of universe with a polytropic equation of state: I. The early universe. *Eur. Phys. J. Plus* **2014**, *129*, 38. [[CrossRef](#)]
27. Chavanis, P.H. Models of universe with a polytropic equation of state: II. The late universe. *Eur. Phys. J. Plus* **2014**, *129*, 222. [[CrossRef](#)]
28. Chavanis, P.H. Models of universe with a polytropic equation of state: III. The phantom universe. *arXiv* **2012**, arXiv:1208.1185.
29. Chavanis, P.H. A cosmological model describing the early inflation, the intermediate decelerating expansion, and the late accelerating expansion of the universe by a quadratic equation of state. *Universe* **2015**, *1*, 357–411. [[CrossRef](#)]
30. Chavanis, P.H. Is the Universe logotropic? *Eur. Phys. J. Plus* **2015**, *130*, 130. [[CrossRef](#)]
31. Chavanis, P.H. The Logotropic Dark Fluid as a unification of dark matter and dark energy. *Phys. Lett. B* **2016**, *758*, 59–66. [[CrossRef](#)]
32. Ferreira, V.M.C.; Avelino, P.P. New limit on logotropic unified dark energy models. *Phys. Lett. B* **2017**, *770*, 213–216. [[CrossRef](#)]
33. Odintsov, S.D.; Oikonomou, V.K.; Timoshkin, A.V.; Saridakis, E.N.; Myrzakulov, R. Cosmological fluids with logarithmic equation of state. *Ann. Phys.* **2018**, *398*, 238. [[CrossRef](#)]

34. Capozziello, S.; D'Agostino, R.; Luongo, O. Cosmic acceleration from a single fluid description. *Phys. Dark Univ.* **2018**, *20*, 1. [[CrossRef](#)]
35. Chavanis, P.H. New predictions from the logotropic model. *Phys. Dark Univ.* **2019**, *24*, 100271. [[CrossRef](#)]
36. Benaoum, H.B.; Luongo, O.; Quevedo, H. Extensions of modified Chaplygin gas from Geometrothermodynamics. *Eur. Phys. J. C* **2019**, *79*, 577. [[CrossRef](#)]
37. Boshkayev, K.; D'Agostino, R.; Luongo, O. Extended logotropic fluids as unified dark energy models. *Eur. Phys. J. C* **2019**, *79*, 332. [[CrossRef](#)]
38. Capozziello, S.; D'Agostino, R.; Giambò, R.; Luongo, O. Effective field description of the Anton-Schmidt cosmic fluid. *Phys. Rev. D* **2019**, *99*, 023532. [[CrossRef](#)]
39. Li, H.; Yang, W.; Gai, L. Astronomical bounds on the modified Chaplygin gas as a unified dark fluid model. *Astron. Astrophys.* **2019**, *623*, A28. [[CrossRef](#)]
40. Chavanis, P.H.; Kumar, S. Comparison between the Logotropic and Λ CDM models at the cosmological scale. *J. Cosmol. Astropart. Phys.* **2017**, *1705*, 018. [[CrossRef](#)]
41. Mamon, A.A.; Saha, S. The logotropic dark fluid: Observational and thermodynamic constraints. *Int. J. Mod. Phys. D* **2020**, *29*, 2050097. [[CrossRef](#)]
42. Boshkayev, K.; Konysbayev, T.; Luongo, O.; Muccino, M.; Pace, F. Testing generalized logotropic models with cosmic growth. *Phys. Rev. D* **2021**, *104*, 023520. [[CrossRef](#)]
43. Donato, F.; Gentile, G.; Salucci, P.; Frigerio Martins, C.; Wilkinson, M.I.; Gilmore, G.; Grebel, E.K.; Koch, K.; Wyse, R. A constant dark matter halo surface density in galaxies. *Mon. Not. R. Astron. Soc.* **2009**, *397*, 1169–1176. [[CrossRef](#)]
44. Chavanis, P.H. Predictions from the logotropic model: The universal surface density of dark matter halos and the present proportions of dark matter and dark energy. *Phys. Dark Univ.* **2022**, *37*, 101098. [[CrossRef](#)]
45. Chandrasekhar, S. *An Introduction to the Theory of Stellar Structure*; University of Chicago Press: Chicago, IL, USA, 1939.
46. Chavanis, P.H. A new logotropic model based on a complex scalar field with a logarithmic potential. *arXiv* **2022**, arXiv:2201.05908.
47. Weinberg, S. *Gravitation and Cosmology*; John Wiley: New York, NY, USA, 2020.
48. Caldwell, R.R. A phantom menace? Cosmological consequences of a dark energy component with super-negative equation of state. *Phys. Lett. B* **2002**, *545*, 23. [[CrossRef](#)]
49. Caldwell, R.R.; Kamionkowski, M.; Weiberg, N.N. Phantom energy: Dark energy with $w < -1$ causes a cosmic doomsday. *Phys. Rev. Lett.* **2003**, *91*, 071301.
50. Frampton, P.H.; Ludwick, K.J.; Scherrer, R.J. The little rip. *Phys. Rev. D* **2011**, *84*, 063003. [[CrossRef](#)]
51. Sandvik, H.; Tegmark, M.; Zaldarriaga, M.; Waga, I. The end of unified dark matter? *Phys. Rev. D* **2004**, *69*, 123524. [[CrossRef](#)]